Bis(pyrazolyl) palladium(II), platinum(II) and gold(III) complexes: Syntheses, molecular structures and substitution reactions with L-cysteine

Frankline K. Keter [a], Stephen O. Ojwach [a], Olayinka A. Oyetunji [b], Ilia A. Guzei [c], James Darkwa [a,*]

[a] Department of Chemistry, University of Johannesburg, P.O. Box 524 Auckland Park 2006, South Africa
[b] Department of Chemistry, University of Botswana, Private Bag UB 00704, Gaborone, Botswana
[c] Department of Chemistry, University of Wisconsin-Madison, 1101 University Avenue, Madison, WI 53706, USA

ARTICLE INFO

Article history:
Received 22 August 2008
Accepted 27 November 2008
Available online 10 December 2008

Keywords:
Bis(pyrazolyl)acetic acid compounds
Cytotoxicity
Pseudo first-order
Substitution
L-cysteine

ABSTRACT

A series of pyrazolyl palladium(II), platinum(II) and gold(III) complexes, $[PdCl_2(3,5\text{-}R_2bpza)]$ {R = H (**1**), R = Me (**2**), bpza = bis-pyrazolyl acetic acid}, $[PtCl_2(3,5\text{-}R_2bpza)]$ {R = H (**3a**), R = Me (**4**)}, $[AuCl_2(3,5\text{-}R_2bpza)]Cl$ {R = H (**5a**), R = Me (**6a**)} and $[PdCl_2(3,5\text{-}R_2bpzate)]$ {R = Me (**7**)} have been synthesised and structurally characterised. Single crystal X-ray crystallography showed that the pyrazolyl ligands exhibit N^N-coordination with the metals. Anticancer activities of six complexes **1**–**6a** were investigated against CHO cells and were found to have low activities. Substitution reactions of selected complexes **1**, **2**, **3a** and **5a** with L-cysteine show that the low anticancer activities compounds and that the rate of substitution with sulfur-containing compounds is not the cause of the low anticancer activities.

1. Introduction

Since the introduction of poly(pyrazolyl)borate as ligands by Trofimenko in the 1970s, pyrazolyl ligands have proven to be popular ligands in coordination chemistry for a wide range of applications. This is because of the ease of synthesis, functionalisation and steric protection they offer to metal centres [1,2]. More recently, a variety of "heteroscorpionate" ligands based on bis(pyrazolyl)methane derivatives containing additional donor atoms, such as O, N and S, have been reported [3,4]. In particular, Otero and co-workers [3a] have shown that by replacing one of the pyrazolyl units in tris(pyrazolyl)methane compounds with a carboxylic group, to obtain bis(pyrazolyl)acetic acid (R_2bpza) ligands, could lead to improved water solubility of the resultant metal complexes. Our interest was therefore to use bis(pyrazolyl)acetic acid compounds as ligands to synthesise water soluble palladium(II), platinum(II) and gold(III) complexes and to investigate their potential anticancer properties.

While it is widely accepted that the anticancer activity of cisplatin and related compounds exerts their activities by interacting with DNA, reactions with other molecules in biological fluids are likely to prevent these compounds from reaching targeted tumour cells [5]. It is thus possible that the sulfur-containing compounds such as L-cysteine could reduce the efficacy of these compounds. On the other hand, there are conflicting reports as to whether gold(III) compounds target DNA or not. Earlier reports implicate gold(III) compounds to bind DNA [6] but these interactions have since been shown to be weak, reversible, and mainly electrostatic in nature, suggesting that DNA is not the primary target for the cytotoxic effects of these gold (III) complexes [7]. A recent report by Milacic and co-workers suggests that proteosome as one of the primary targets for gold(III) compounds [8].

Substitution reactions performed with d^8 platinum(II) complexes are slower than other square-planar complexes [9]. For instance cisplatin kinetics with L-cysteine is bimolecular with a slow rate constant of $2.2 \pm 0.2 \times 10^{-2}\,M^{-1}\,s^{-1}$ at 37 °C [10] while gold(III) complexes react *ca.* 10^3 times faster and palladium(II) complexes react *ca.* 10^5–10^6 times faster [11,12]. Gold(III) and palladium(II) compounds are also kinetically unstable [9]. Gold(III) compounds in particular are known to be unstable and easily reduce to gold(I) under physiological conditions due to their rapid kinetics and high redox potential [13]. Using bis(pyrazolyl)acetic acid, we have shown that these ligands can stabilise both palladium(II) and gold(III) enough to allow their kinetics to be studied.

2. Experimental

2.1. Materials and instrumentation

All commercial chemicals and other reagents other than those described were used as received. L-cysteine was purchased from Sigma–Aldrich and used with no further purification. The palladium and gold starting materials, $[PdCl_2(NCMe)_2]$ [14] and

* Corresponding author. Tel.: +27 11 559 2838.
E-mail address: jdarkwa@uj.ac.za (J. Darkwa).

$H[AuCl_4]\cdot 4H_2O$ [15], were synthesised according to the literature procedures, respectively. Bis(pyrazolyl)acetic acid (**L1**) and bis(3,5-dimethylpyrazolyl)acetic acid (**L2**) were also synthesised according to the literature methods [16]. The water used was double distilled. All manipulations of air-and/or moisture sensitive compounds were performed using Schlenk techniques. IR spectra were recorded as nujol mulls and as KBr pellets on a Perkin–Elmer, paragon 1000 FTIR spectrophotometer. ^1H and $^{13}C\{^1H\}$ NMR spectra were recorded on a Gemini 2000 instrument (200 MHz) and a Bruker Avance DPX 300 spectrometer (300 MHz) in $CDCl_3$ and DMSO-d_6. ^1H chemical shifts were referenced to the signals of the residual protons of the NMR solvents and are quoted in ppm. Mass spectrometry data were recorded on a Waters API Quattro Micro spectrophotometer. Kinetic studies were performed using a Shimadzu UV-2501PC UV-Vis spectrophotometer and a Hi-Tech SF-61 DX2 stopped-flow spectrophotometer.

2.2. Reagents for screening of biological activity of complexes

All reagents, other than those described, were used as received. All cell culture reagents were supplied by Invitrogen Ltd. and cisplatin by Sigma–Aldrich. The Hams F-12 medium containing 10% foetal calf serum and 0.2% pn-streptomycin was prepared from the stock Hams F-12 medium. The solutions of the six palladium(II), platinum(II) and gold(III) complexes **1–6a** screened, were prepared as 10 mM stock solutions.

2.3. Synthesis of ligands *L3*, *L4* and metal complexes

2.3.1. Bis(pyrazol-1-yl)ethyl acetate (*L3*)

Ligand **L1** (0.50 g, 2.60 mmol) was refluxed for 18 h in excess ethanol (40 mL) under acidic conditions (HCl, 5 mL). The mixture was cooled to room temperature, 50 mL of deionised water added and the pH adjusted to 11 using sodium hydrogen carbonate. The organic phase was extracted using dichloromethane (50 mL) and dried over $MgSO_4$. The solvent was then removed *in vacuo* to afford an analytically pure white crystalline material of. Yield = 0.33 g (58%). ^1H NMR ($CDCl_3$): δ 7.74 (d, 2H, pz, $^3J_{HH}$ = 2.2 Hz, 5-pz); 7.59 (t, 2H, pz, $^3J_{HH}$ = 1.6 Hz, 3-pz); 7.10 (s, 1H, $CHCO_2H$); 6.33 (t, 2H, pz $^2J_{HH}$ = 1.8 Hz, 4-pz); 4.34 (q, 2H, Et, $^3J_{HH}$ = 7.4 Hz); 1.26 (t, 3H, Et, $^3J_{HH}$ = 7.4 Hz); $^{13}C\{^1H\}$NMR ($CDCl_3$): δ 163.8 (C(C=O)); 140.4 (C(5-pz); 129.6 (C(3-pz)); 106.8 (C(4-pz)); 74.1 (C($CHCO_2H$)); 62.7 (C(CH_2, Et)); 13.4 (C(CH_3, Et)). EIMS (70 eV). *m/z* 221 (2%) [M^+]. IR (Nujol, cm^{-1}): 1750 ($\nu_{C=O}$). *Anal.* Calc. for $C_{10}H_{12}N_4O_2$: C, 54.54; H, 5.49; N, 25.44. Found: C, 54.36; H, 5.75; N, 25.09%.

2.3.2. Bis(3,5-dimethylpyrazol-1-yl)ethyl acetate (*L4*)

The synthesis of **L4** was performed in a similar manner as described for **L3** by using **L2** (1.50 g, 2.60 mmol). Yield = 0.90 g (58%). ^1H NMR ($CDCl_3$): δ 7.10 (s, 1H, $CHCO_2H$); 5.84 (s, 1H, 4-pz); 4.26 (q 2H, Et, $^2J_{HH}$ = 7.4 Hz); 2.41 (s, 6H, CH_3, 3-pz); 2.34 (s, 6H, CH_3, 5-pz); 1.30 (t, 3H, Et, $^2J_{HH}$ = 7.4 Hz);. $^{13}C\{^1H\}$NMR ($CDCl_3$): δ 166.1 (C(C=O)); 147.0 (C(5-pz); 140.8 (C(3-pz)); 106.6 (C(4-pz)); 71.7 (C($CHCO_2H$)); 63.2 (C(CH_2, Et)); 13.4 (C(CH_3, Et)); 12.8 (C(CH_3, 5-pz)); 11.0 (C(CH_3, 3-pz)). IR (Nujol, cm^{-1}): 1735 ($\nu_{C=O}$). EI-MS (70 eV); *m/z* 276 (5%) [M^+]. *Anal.* Calc. for $C_{14}H_{20}N_4O_2$: C, 60.85; H, 7.30; N, 20.28. Found: C, 60.76; H, 7.55; N, 19.98%.

2.3.3. Dichloro-(bis(pyrazol-1-yl)acetic acid)palladium(II) (*1*)

To a yellow solution of $K_2[PdCl_4]$ (0.17 g, 0.52 mmol) in distilled water (15 mL), was added **L1** (0.10 g, 0.52 mmol) and the mixture stirred vigorously at room temperature. After 1.5 h, a colour change from a yellow solution to an orange suspension was observed and further stirring for 3 h resulted in the formation of a yellow precipitate. The precipitate was isolated by filtration and washed with ethanol to afford pure **1**. Yield = 0.15 g; (75%). ^1H NMR (DMSO-d_6) δ 8.29 (d, 2H, $^2J_{HH}$ = 1.8 Hz, 5-pz); 8.14 (s, 1H, $CHCO_2H$); 8.02 (d, 2H, $^2J_{HH}$ = 1.8 Hz, 3-pz); 6.63 (t 2H, $^2J_{HH}$ = 2.6 Hz, 4-pz). $^{13}C\{^1H\}$ NMR: (DMSO-d_6): δ 164.9 (C(C=O)); 144.4 (C(5-pz); 136.9 (C(3-pz)); 108.0 (C(4-pz)); 72.2 (C($CHCO_2H$)). IR (Nujol, cm^{-1}): 3441 (ν_{O-H}), 1738 ($\nu_{C=O}$). *Anal.* Calc. for $C_8H_8Cl_2N_4O_2Pd$: C, 26.00; H, 2.18; N, 15.16. Found: C, 26.34; H, 2.22; N, 15.20%.

2.3.4. Dichloro(bis(3,5-dimethylpyrazol-1-yl)acetic acid)palladium(II) (*2*)

Compound **2** was prepared from a mixture of **L2** (0.10 g, 0.40 mmol) and $[PdCl_2(NCMe)_2]$ (0.10 g, 0.38 mmol) in CH_2Cl_2 (20 mL). The mixture was stirred for 6 h upon which a yellow precipitate was formed. The precipitate was isolated by filtration, washed with minimum amount of ethanol and the solid dried in air to afford an analytically pure product. Yield = 0.10 g; (63%). ^1H NMR: (DMSO-d_6): δ 6.04 (s, 2H, 4-pz); 5.61 (s, 1H, $CHCO_2H$); 2.42 (s, 6H, 5-pz); 2.31 (s, 6H, 3-pz). $^{13}C\{^1H\}$ NMR: (DMSO-d_6): δ 165.3 (C(C=O)); 149.2 (C(5-pz); 145.7 (C(3-pz)); 106.2 (C(4-pz)); 72.6 (C($CHCO_2H$)); 13.6 (C(3-CH_3)); 12.9 (C(CH_3, 3-pz)). IR (Nujol, cm^{-1}) 3410 (ν_{O-H}), 1756 ($\nu_{C=O}$). *Anal.* Calc. for $C_{12}H_{16}Cl_2N_4O_2Pd\cdot 0.5CH_2Cl_2$: C, 32.25; H, 3.23; N, 12.04. Found: C, 32.27; H, 3.41; N, 12.25%.

2.3.5. Dichloro(bis(pyrazol-1-yl)acetic acid)platinum(II) (*3a*)

To a red solution of $K_2[PtCl_4]$ (0.43 g, 1.00 mmol) in distilled water (15 mL), was added **L1** (0.20 g, 1.00 mmol) and the mixture vigorously stirred at room temperature. After 1.5 h a colour change from a red solution to an orange suspension was observed and further stirring resulted in the formation of a yellow precipitate. The product was isolated as a precipitated. Yield: **3a** 0.25 g (52%). ^1H NMR: (DMSO-d_6): δ 8.34 (d, 2H, $^3J_{HH}$ = 2.20 Hz, 5-pz); 8.12 (d, 2H, $^3J_{HH}$ = 4.80 Hz, 3-pz); 7.96 (s, 1H, $CHCO_2H$); 6.65 (t, 2H, $^2J_{HH}$ = 1.8 Hz, 4-pz). $^{13}C\{^1H\}$ NMR: (DMSO-d_6): δ 166.2 (C(C=O)); 140.1 (C(5-pz); 131.0 (C(3-pz)); 106.5 (C(4-pz)); 73.9 (C($CHCO_2H$)). IR (Nujol, cm^{-1}): 3460 (ν_{O-H}), 1763 ($\nu_{C=O}$), 1517 ($\nu_{C=N}$). ESI-MS: *m/z* 457 (10%) [$PtCl_2$(bpza)]$^+$ (10%), *m/z* 490 [$PtCl_2$(bpza)+Na]$^+$ (20%). *Anal.* Calc. for $C_8H_8Cl_2N_4O_2Pt$ (**3a**): C, 20.97; H, 1.76; N, 12.23. Found: C, 20.67; H, 1.60; N, 12.29%.

2.3.6. $K_2[Pt_4Cl_8(L1^-)_2(L1)_2]\cdot 2H_2O$ (*3b*)

After isolation of **3a**, the filtrate was left to stand for 1 day upon which golden yellow single crystals of **3b** suitable for X-ray analysis were formed. *Anal.* Calc. for $K_2[C_{32}H_{34}Cl_8N_{16}O_{10}Pt_4]$ (**3b**): C, 19.76; H, 1.76; N, 11.52. Found: C, 19.68; H, 1.65; N, 11.89%.

2.3.7. Dichloro(bis(3,5-dimethylpyrazol-1-yl)acetic acid)platinum(II) (*4*)

The synthesis of this compound was performed in a similar manner as described for **3a**. $K_2[PtCl_4]$ (0.37 g, 0.81 mmol) and bis(3,5-dimethylpyrazol-1-yl)acetic acid (0.20 g, 0.81 mmol). Yield: 0.38 g (75%). ^1H NMR: (DMSO-d_6): δ 7.13 (s, 1H, $CHCO_2H$); 5.86 (s, 2H, 4-pz); 2.17 (s, 6H, 5-pz); 2.07 (s, 6H, 3-pz). $^{13}C\{^1H\}$ NMR: (DMSO-d_6): δ 165.9 (C(C=O)); 146.8 (C(5-pz); 140.5 (C(3-pz)); 106.4 (C(4-pz)); 71.4 (C($CHCO_2H$)); 13.2 (C(CH_3, 5-pz)); 10.8 (C(CH_3, 3-pz)). IR (Nujol cm^{-1}): 3439 (ν_{O-H}), 1743 ($\nu_{C=O}$), 1560 ($\nu_{C=N}$). ESI-MS: *m/z* 519 [$PtCl_2$(3,5-Me_2bpza)]$^+$ (10%). *Anal.* Calc. for $C_{12}H_{14}Cl_2N_4O_2Pt$: C, 28.03; H, 3.14; N, 10.89. Found: C, 27.72; H, 3.25; N, 10.80%.

2.3.8. Dichloro(bis(pyrazol-1-yl)acetic acid gold(III) chloride (*5a*)

To a solution of $H[AuCl_4]\cdot 4H_2O$ (0.18 g, 0.52 mmol) in distilled water (10 mL) was added **L1** (0.10 g, 0.52 mmol) and resulted in an immediate formation of a yellow precipitate. The reaction mixture was stirred for 45 min at room temperature. The product was isolated by filtration and dried *in vacuo*. Yield: 0.15 g (63%). ^1H NMR(DMSO-d_6): δ 8.47 (m, 4H, 5-pz, 3-pz); 8.11 (1H, $CHCO_2H$);

6.95 (m, 2H, 4-pz). $^{13}C\{^1H\}$ NMR(DMSO-d_6): 174.3 (C(C=O)); 149.4 (C(5-pz); 140.2 (C(3-pz)); 115.9 (C(4-pz)); 83.2 (C($CHCO_2H$)). IR (KBr, cm^{-1}): 3492 (ν_{O-H}), 1761 ($\nu_{C=O}$), 1509 ($\nu_{C=N}$). ESI-MS: *m/z* 463 $[AuCl_2(bpza)]^+$ (5%). *Anal.* Calc. $C_8H_8AuCl_3N_4O_2$: C, 24.39; H, 2.52; N, 9.42. Found: C, 24.53; H, 2.87; N, 9.53%.

2.3.9. Dichloro(bis(3,5-dimethylpyrazolyl)acetic acid)gold(III)chloride (**6a**)

The synthesis of **6a** was performed in a similar manner as described for **5a**. $H[AuCl_4]\cdot 4H_2O$ (0.10 g, 0.30 mmol) and bis(3,5-dimethylpyrazol-1-yl)acetic acid (0.07 g, 0.30 mmol). Yield: 0.09 g (59%). ^1H NMR (DMSO-d_6): δ 7.15 (s, 1H, $CHCO_2H$); 5.88 (s, 2H, 4-pz); 2.18 (s, 6H, 5-pz); 2.08(s, 6H, 3-pz). $^{13}C\{^1H\}$ NMR(DMSO-d_6): 165.8 (C(C=O)); 146.9 (C(3-pz); 140.6 (C(4-pz)); 106.4 (C(5-pz)); 71.1 (C($CHCO_2H$)); 13.1 (C(CH_3, 5-pz)); 10.7 (C(CH_3, 3-pz)). IR (KBr cm^{-1}): 3451 (ν_{O-H}), 1765 ($\nu_{C=O}$), 1518 ($\nu_{C=N}$). ESI-MS: *m/z* 519 $[AuCl_2(3,5\text{-}Me_2bpza)]^+$ (5%). *Anal.* Calc. for $C_{12}H_{14}AuCl_3N_4O_2$: C, 26.13; H, 2.92; N, 10.16. Found: C, 25.70; H, 3.06; N, 9.99%.

2.3.10. Dichloro(bis(3,5-dimethylpyrazol-1-yl)ethyl acetate)palladium(II) (**7**)

The synthesis of **7** was performed in a similar manner as described for **2**. Yield = 0.35 g (58%). ^1H NMR ($CDCl_3$): δ 7.22 (s, 1H, $CHCO_2Et$); 5.90 (s, 1H, 4-pz); 4.31 (q, 2H, Et, $^2J_{HH}$ = 7.4 Hz); 2.47 (s, 6H, CH_3, 5-pz); 2.25 (s, 6H, CH_3, 3-pz); 1.35 (t, 3H, Et, $^2J_{HH}$ = 7.4 Hz). $^{13}C\{^1H\}$ NMR ($CDCl_3$): δ 168.5 (C(C=O)); 145.7 (C(5-pz); 141.5 (C(3-pz)); 107.1 (C(4-pz)); 70.9 (C($CHCO_2H$)); 62.4 (C(CH_2)); 13.6 (C(CH_3))13.4 (C(3-CH_3)); 10.0 (C(5-CH_3)). IR (Nujol, cm^{-1}): 1741 ($\nu_{C=O}$). *Anal.* Calc. for $C_{14}H_{20}Cl_2N_4O_2Pd$: C, 37.07; H, 4.44; N, 12.35. Found: C, 37.48; H, 4.05; N, 12.62%.

2.4. X-ray crystallography

Crystals of compounds **L4**, **1**, **3b** and **5b** were mounted in oil on a glass fiber and data collection performed on a Bruker CCD-1000 diffractometer with Mo Kα (λ = 0.71073 Å) radiation and the diffractometer to crystal distance of 4.9 cm. The reflections were successfully indexed by an automated indexing routine built in the SMART program. These highly redundant datasets were corrected for Lorentz and polarisation effects. The absorption correction was based on fitting a function to the empirical transmission surface as sampled by multiple equivalent measurements. A successful solution by the direct methods provided all non-hydrogen atoms from the *E*-map. All non-hydrogen atoms were refined with anisotropic displacement coefficients. All hydrogen atoms were included in the structure factor calculation at idealised positions and were allowed to ride on the neighbouring atoms with relative isotropic displacement coefficients [17].

2.5. Cell culture and treatment

The anticancer activities of **1–6a** were tested on exponentially dividing CHO cells according to the neutral red (NR) dye assay [18]. CHO cells were cultured in 96 well plates at a population of 2×10^4 cells per well using Hams F-12 medium. After a 24 h pre-incubation period, at 37 °C, 5% CO_2 atmosphere, the cells were washed with phosphate buffered saline (PBS). Fresh Ham F-12 medium (100 μL) containing the test compounds was added and incubated for 24 h. The cells were then washed twice with PBS and 100 μL of serum free Ham F-12 medium containing NR dye (100 μg/mL) was added to the cells and incubated for 3 h. The cells were then washed twice with PBS and 50 μL of an elution buffer (ethanol:acetic acid:water (50%:1%:49%)) used to lyse the cells and the accumulated NR dye measured in a multi-well spectrophotometer [18,19].

2.6. Kinetics experiments

In a typical kinetic study an aqueous solution of **11** was prepared by the addition of 2.99 molar equivalents of $AgClO_4$ to 0.2% DMSO solution of **5** in 0.1 M $HClO_4$, while aqueous solutions of **8–10** were prepared by addition of 1.99 molar equivalents of $AgClO_4$ at the same ionic strength. The resulting solution of **8–11** was filtered using a 0.5 μm Miller-LCR filter and made up to 50 mL to obtain the desired concentration of stock solution. Temperatures were maintained to an accuracy of ±0.1 °C while the ionic strength was maintained at 0.10 M $HClO_4/LiClO_4$ in all the reactions monitored. Kinetic measurements were obtained at fixed wavelengths of maximum absorbance, namely: 315 nm for the palladium(II) complex, 285 nm for the platinum(II) complex and 239 nm for the gold(III) complex. Preliminary investigations showed that the reactions were inversely dependent on acidity. Thus all reactions were studied at pH range of 2.92–3.72 to guarantee the presence of diaqua form of the complexes [20]. The kinetics was followed under pseudo first-order conditions with the L-cysteine concentrations in large excess over those of the complexes (10:1; [Cys]:[complex]). All kinetic studies were followed for at least 4 half-lives. For slow processes, the pseudo first-order rate constants, k_{obs}, were obtained by importing absorbance changes data from the UV–Vis spectrophotometer into the single exponential fitting of the KINETASYST™3 software programme of the stopped-flow equipment. The k_{obs} values for fast processes were obtained directly from the stopped-flow equipment software programme (KINETASYST™3) by fitting the curves to single exponential analysis. All reactions were studied between 298 and 313 K.

Caution: Perchlorate salts of metal complexes with organic ligands are potentially explosive.

3. Results and discussion

3.1. Synthesis of metal complexes

The metal complexes $[PdCl_2(L)]$ {**L** = **L1** (**1**), **L2** (**2**)}, $[PtCl_2(L)]$ {**L** = **L1** (**3a**), **L2** (**4**)} and $[AuCl_2(L)]Cl$ {**L** = **L1** (**5a**), **L2** (**6**)} were prepared by reacting bis(pyrazolyl)acetic acid (**L1**) or bis(3,5-dimethylpyrazolyl)acetic acid (**L2**) with equimolar amounts of $K_2[PdCl_4]$ or $K_2[PtCl_4]$ and/or $H[AuCl_4]\cdot 4H_2O$ (Scheme 1). These metal complexes were characterised by a combination of NMR, mass spectrometry and in selected cases by single crystal X-ray crystallography. A typical ^1H NMR spectrum is that of **1** which showed three distinct singlets at 8.29 ppm (5H, 5′H), 8.02 ppm (3H, 3′H) of the pyrazolyl units and at 8.14 ppm for the CH linker proton (*CH*COOH) as compared to two broad peaks at 7.97 and 7.56 ppm in the spectrum of **L1** for all the five protons. The ^1H NMR spectra of **2**, **4** and **6a** showed distinct separation of the two methyl groups of the pyrazolyl units in the range 2.07–2.42 ppm as compared to the two methyl groups in **L2** that overlap at 2.33 ppm. Complexes **3a**, **4**, **5a** and **6a** were further characterised by mass spectrometry. All complexes gave the expected molecular ions. Complexes **5a** and **6a** formed cationic gold(III) complexes with chloride counterion and are similar to $[AuCl_2(bik)]Cl$ and $[AuCl_2(bihm)]Cl$ (bik = bis(1-methyl-2-imidazolyl)ketone, bihm = bis(1-methyl-2-imidazolyl)hydroxymethane) complexes recently reported by Bulak et al. [21].

3.2. Molecular structures of complexes *1* and *3b*

Single crystals of palladium(II) complex **1** were grown by slow evaporation of an aqueous solution at room temperature, but single crystals of platinum(II) complex $K_2[Pt_4Cl_8(\mathbf{L1}^-)_2(\mathbf{L1})_2]\cdot 2H_2O$ (**3b**) were obtained from the reaction mixture used in the synthesis

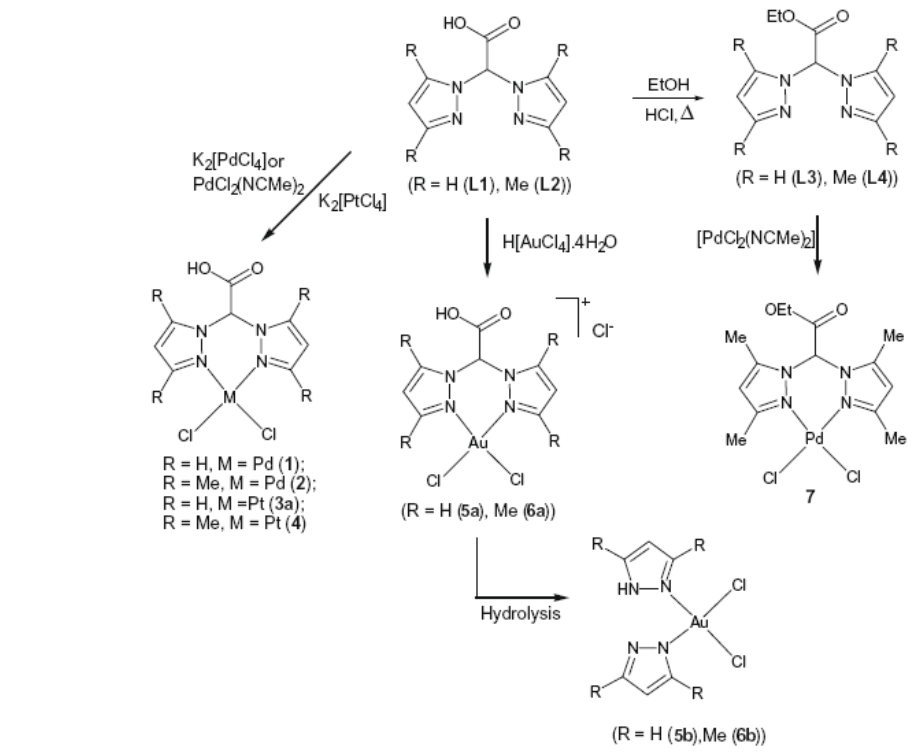

Scheme 1.

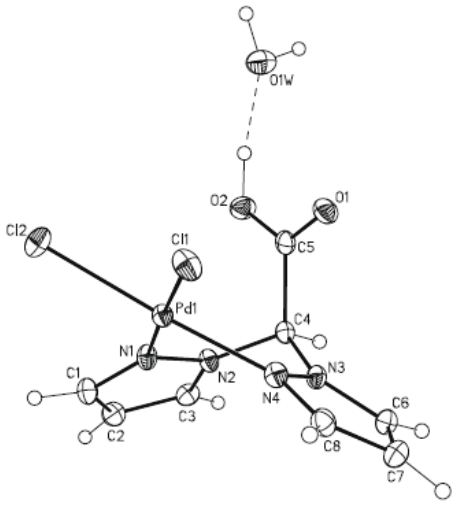

Fig. 1. A molecular drawing of **1**. The hydrogen bonding interaction is shown with a dash line.

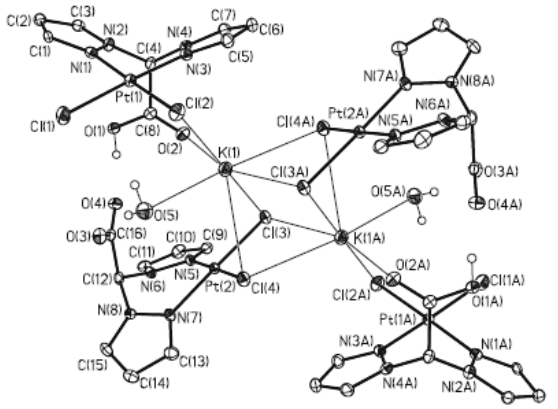

Fig. 2. Hexanuclear complex **3b** with four platinum atoms and two potassium atoms. Selected H atoms are shown.

of [$PtCl_2$(**L1**)] (**3a**). The molecular structures of complexes **1** and **3b** are shown in Figs. 1 and 2, respectively and Tables 1 and 2 show the crystallographic data, and selected bond lengths and angles, respectively. In complex **1** the two chlorides are coordinated to palladium in a *cis*-arrangement with a distorted square-planar geometry. The N(1)–Pd(1)–N(4), N(4)–Pd(1)–Cl(1), N(1)–Pd(1)–Cl(2) bond angles are 88.03(6)°, 90.04(4)° and 90.81(4)°), respectively. The average Pd–Cl bond distances of **1** is 2.2866(5) Å and is similar to the average Pd–Cl distance of 2.301 Å reported to the Cambridge Structural Database (CSD) [22]. However, the

Table 1
Crystal data and structure refinement for **L4**, **1**, **3b** and **5b**.

Parameter	L4	1	3b	5b
Formula	$C_{14}H_{20}N_4O_2$	$C_{58}H_{10}Cl_2N_4O_3Pd$	$C_{32}H_{34}Cl_8K_2N_{16}O_{10}Pt_4$	$C_6H_7AuCl_2N_4$
Formula weight	276.34	387.50	1944.91	403.02
Temperature (K)	100(2)	105(2)	100(2)	100(2)
Wavelength (Å)	0.71073	0.71073	0.71073	0.71073
Crystal system	triclinic	monoclinic	monoclinic	monoclinic
Space group	*P*1	$P2_1/n$	$P2_1/n$	*C*2/*c*
a (Å)	8.4121(18)	10.9934(10)	10.7762(8)	9.1848(6)
b (Å)	8.7475(19)	9.7436(9)	14.4036(11)	14.8376(10)
c (Å)	10.809(2)	11.9243(11)	16.6971(13)	14.9738(10)
α (°)	80.958(3)	90	90	90
β (°)	71.135(3)	93.0620(10)	104.494(2)	100.9060(10)
γ (°)	84.365(3)	90	90	90
Volume (Å^3)	742.4(3)	1275.5(2)	2509.2(3)	2003.8(2)
Z	2	4	2	8
D_{calcd} (mg/m^3)	1.236	2.021	2.574	2.672
Absorption coefficient (mm^{-1})	0.085	1.882	11.777	15.174
F(000)	296	760	1808	1472
Final *R* indices (R_1)	0.0587	0.0180	0.0205	0.0172
Reflections collected	6053	20998	20392	13947
Completeness to theta (%)	98.1	100	99.7	98.4
Goodness-of-fit (GOF) on F^2	1.051	1.057	1.023	1.075
Largest difference peak and hole (e Å^{-3})	1.337 and −0.218	0.523 and −0.370	1.234 and −0.792	1.401 and −02.024

Table 2
Selected bond lengths [Å] and angles [°] for **1** and **3b**.

	1 M = Pd	3b M = Pt
Bond lengths (Å)		
M(1)–N(1)	2.007(4)	2.005(3)
M(1)–N(3)	2.031(4)	2.016(3)
M(1)–Cl(1)	2.2803(13)	2.2909(10)
N(1)–N(2)	1.366(6)	1.359(4)
O(1)–C(5)	1.204(2)	
O(2)–C(8)		1.215(5)
O(3)–C(16)		1.224(5)
K(1)–Cl(2)		3.1822(13)
Pt(1)–K(1)		3.8397(9)
Bond angles (°)		
N(1)–M(1)–N(3)	87.39(17)	90.11(13)
N(1)–M(1)–Cl(2)	177.63(12)	177.87(9)
N(1)–M(1)–Cl(1)	91.07(12)	89.11(9)

average Pd–N bond distance (2.0131(15) Å) is shorter than the average Pd–N bond distance of 2.06(9) Å for 607 bonds in 229 relevant complexes reported to the CSD [22].

The structure of complex **3b**, a hexanuclear centrosymmetric complex, consists of four independent platinum(II) complexes, each with a platinum centre that has a slightly distorted square-planar geometry. Only one half of it is crystallographically independent. Each platinum coordination environment consists of two *cis*-Cl ligands and one K^2-N^N$_{(L1)}$ unit. Two of the platinum moieties in complex **3b** have deprotonated carboxylic acid units and two K^+ counter ions. Interestingly, the pyrazolyl rings in the bpza and deprotonated bpza units are not coplanar. The platinum coordination sphere and the six-membered heterocycle Pt–N–N–C–N–N adopt a boat conformation which in this structure resembles a butterfly that has a dihedral folding angle along the Pt···C(N,N) line averaging 48.7(2)° for the two crystallographically independent complexes. In the centre of complex **3b** is a K_2Cl_4 fragment that has a shape of a trigonal antiprism. Each potassium atom is seven-coordinate forming bonds to five Cl atoms from three platinum complexes, one oxygen atom belonging to a carboxylic acid unit, and a solvent water molecule. The coordination environment about K(1) is a distorted capped trigonal prism (the trigonal prism is formed by facets C(13)–C(14)–O(5) and C(12)–C(13A)–C(14A) and capped with O(2). Atom K(1) forms ionic distal interactions of various lengths with the Cl and O atoms, which is typical for potassium cations. Each potassium atom is also part of two K–Cl–K–Cl four-membered rings, two K–Cl–Pt–Cl four-membered rings, and two 8-membered K–Cl–Pt–N–N–C–C–O rings. While there are several intramolecular O–H···O hydrogen bonding interactions within complex **3b**, there are no intermolecular interactions in its lattice.

3.3. Acidity of ligands and palladium(II) complex

Having observed dissociation of carboxylic acid in platinum(II) complex **3a**, we investigated the acidity of **L1**, **L2** and those of their palladium(II) complexes by pH titration experiments (Fig. S1). The acidity of palladium(II) complexes was investigated primarily because these complexes did not readily dissociate when water was added compared to the platinum(II) analogues. The pH titrations were performed using 0.1 M NaOH. The K_a of **L1** is 9×10^{-3} ($pK_a = 2.04$), whilst that of **L2** is 2.0×10^{-4} ($pK_a = 3.70$), indicating that the methyl substituents on **L2** significantly reduces its acidity. The K_a of acetic acid is 1.8×10^{-4} value ($pK_a = 4.76$) [23], implying that **L1** is more acidic than acetic acid but **L2** has comparable acidity to acetic acid. To establish the effect on the acidity of these ligands on complexation, the K_a of complex **2** was determined. The K_a of complex **2** was found to be 1.30×10^{-2} ($pK_a = 2.0$), which demonstrates the effect of electron donation from the ligand to the metal centre; thus leading to the increased acidity of the carboxylic functionality in the complex.

The acidic nature of **L1** and **L2** was further proved by esterification experiments of **L1** and **L2** to bis(pyrazolyl)ethyl acetate (**L3**) and bis(3,5-dimethylpyrazolyl)ethyl acetate (**L4**), respectively (Scheme 1). The molecular structure of **L4** was determined by X-ray crystallography (Fig. 3). The crystallographic data together with selected bond lengths and angles are given in Tables 1 and 3, respectively. The carbonyl carbon, C(7), exhibits a distorted trigonal geometry. However, around C(6), it is a distorted tetrahedral geometry. The angles vary from 106.2° to 112.49(17)°. The bond distances and angles are within the expected range and are similar to those reported by Burzlaff and co-workers (C(4)–N(12) = 1.468(3) Å, C(5)–O(5) = 1.215(3) Å; O(4)–C(5)–O(5) = 125.4(2)°, C(5)–C(4)–N(22) = 109.2(2)°) for bis(3,5-ditertbutylpyrazolyl)acetic acid [16]. The ability of these ethyl acetate ligands to form complexes was demonstrated by reacting **L4** and $[PdCl_2(MeCN)_2]$ which gave $[PdCl_2(\mathbf{L4})]$ (**7**).

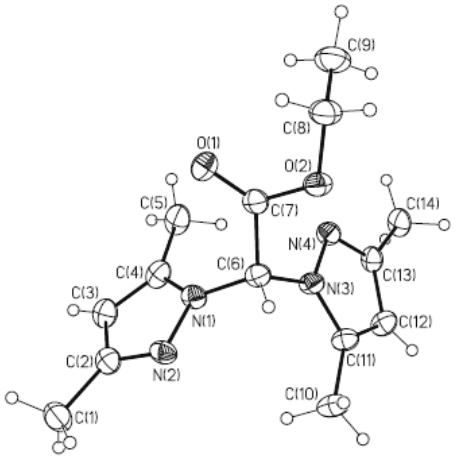

Fig. 3. A molecular drawing of **L4**.

Table 3
Selected bond lengths [Å] and angles [°] for **L4**.

Bond lengths (Å)		Bond angles (°)	
L4			
C(6)–C(7)	1.534(3)	O(1)–C(7)–O(2)	126.3(2)
O(2)–C(7)	1.328(3)	N(1)–C(6)–C(7)	112.49(17)
O(1)–C(7)	1.198(3)	N(1)–C(6)–N(3)	113.75(17)
N(1)–C(6)	1.447(3)		

3.4. Hydrolysis of gold(III) complexes

Attempts to obtain single crystals of $[AuCl_2(\mathbf{L1})]Cl$ (**5a**) led to the formation of a hydrolysed product, $[AuCl_2(pz)(pzH)]$ (**5b**), as confirmed by X-ray crystallography. The ^1H NMR spectrum (Fig. S2a) of complex **5a** showed three peaks centred at 7.56 ppm that account for the 3H, 3′H of the pyrazolyl units as well as the CH linker proton (Fig. S2a). However, the ^1H NMR spectrum of crystals of complex **5b** showed only one broad peak at 7.15 ppm (Fig. S2b). The spectroscopic data as well as the solid state structure of complex **5b** indicate that complex **5a** slowly hydrolysed in solution to produce **5b**. Similarly, **6a** hydrolysed to **6b** (Fig. S3). Recently Cao et al. [24] reported the amine-amide hydrolysis of a gold(III) compound that was attributed to the high polarising nature of the gold(III) centre in this compound. Several reports on the polarising effect of gold(III) have appeared in the literature [25,26]. A similar polarising effect of gold(III) in complexes **5a** and **6a** could explain the hydrolysis we observed.

The molecular structure of complex **5b** is shown in Fig. 4. The crystallographic data are shown in Table 1, whilst the selected bond lengths and angles are shown in Table 4. The bond distances, Au(1)–N(1) (1.998(2) Å), Au(1)–N(3) (2.002(2) Å), Au(1)–Cl(1) (2.3033(6) Å) and Au(1)–Cl(2) (2.2933(7) Å) are longer compared to those reported for dichloro-picolinaminatogold(III) complex (Au(1)–N(2); (1.969(5) Å and Au(1)–Cl(1); (2.2971(14) Å) by Fan et al. [26]. The average Au–N bond distance is also considerably shorter than Au–N distances in $[Au(dmtc)(damp)]BPh_4$ (dmtc = $(CH_3)_2NCS_2$, damp = o-$C_6H_4CH_2$-$N(CH_3)_2$) complex [26]. This is as a result of delocalisation of the π-electrons in the pyrazolyl ring. In addition to the two N atoms of the ligand, Au atom is coordinated to two chlorine atoms. The bond angles, N(1)–Au(1)–N(3) (86.77(9)°); Cl(2)–Au(1)–Cl(1) (90.73(2)°); N(3)–Au(1)–Cl(2) (89.89(7)°) and N(1)–Au(1)–Cl(1) (92.59(7)°) indicate a distorted square-planar geometry with a AuN_2Cl_2 coordination sphere. Coordination around the metal is close to linearity along N(1)–Au(1)–Cl(2) (176.64°) and N(3)–Au(1)–Cl(1) (177.99°).

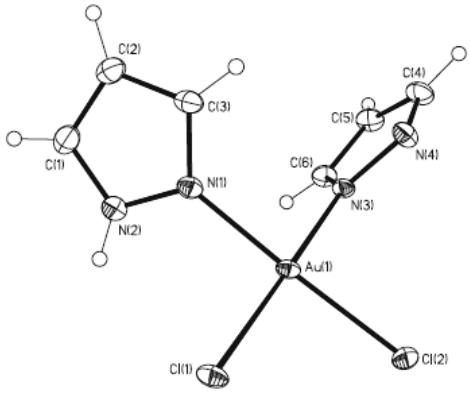

Fig. 4. A molecular drawing of **5b**, with only one position of the hydrogen equally disordered between N(2) and N(4) is shown.

Table 4
Selected bond lengths [Å] and angles [°] for **5b**.

Bond lengths (°)		Bond angles (°)	
5b			
Au(1)–N(1)	1.998(2)	N(1)–Au(1)–N(3)	86.77(9)
Au(2)–N(3)	2.002(2)	N(1)–Au(1)–Cl(2)	176.63(7)
Au(1)–Cl(1)	2.2033(6)	N(1)–Au(1)–Cl(1)	92.59(7)
N(1)–N(2)	1.353(3)		

3.5. Anticancer activity of complexes *1–6a*

Six complexes, **1–6a**, were investigated for their anticancer activities against chinese hamster ovary (CHO) cells at various concentrations (0.025–8 mM). A summary of the IC_{50} values are given in Table 5. The IC_{50} values of complexes **1–6a** were found to be higher than that of cisplatin (0.07 mM). A possibly reason for the low anticancer activity is that these compounds could be reacting faster with sulfur-containing molecules in the biological matrix and hence deactivating. Substitution reaction of selected complexes with L-cysteine was therefore used to probe the possibility of the reaction rates of **1–6a** with sulfur-containing molecules contribute to their observed low anticancer activities.

3.6. Kinetics of L-cysteine reactions with complexes

Substitution reactions of L-cysteine with **1**, **2**, **3a** and **5a** were studied. The kinetics of the chloro complexes **1**, **2**, **3a** and **5a** were very slow, so their diaqua forms, $[Pd(\mathbf{L1})(OH_2)_2]^{2+}$ (**8**), $[Pd(\mathbf{L2})(OH_2)_2]^{2+}$ (**9**), $[Pt(\mathbf{L1})(OH_2)_2]^{2+}$ (**10**) and $[Au(\mathbf{L1})(OH_2)_2]^{3+}$ (**11**) were generated and used in the kinetics. While the reaction

Table 5
Growth inhibition values of compounds **1–6a** tested against CHO cells.

Compound	IC_{50} (mM)	Compound	IC_{50} (mM)
1	1.5 ± 0.2	**4**	4.0 ± 1.2
2	1.1 ± 0.2	**5a**	1.5 ± 0.1
3a	1.5 ± 0.1	**6a**	5.1 ± 0.1
Cisplatin	0.07 ± 0.01		

IC_{50} is the concentration of compounds required to inhibit cell growth by 50%.

Table 6
Second order rate constants for the reaction of L-cysteine with **8**, [Pd(II)] = 3.8 × 10^{-5} M; **9**, [Pd(II)] = 3.8 × 10^{-5} M; **10**, [Pt(II)] = 5 × 10^{-5} M; and **11**, [Au(III)] = 5 × 10^{-5} M; I = 0.1 M, T = 298 K.

T (K)	k_1 (M^{-1} s^{-1})				
	8	**9**	**10**	**11**	Reduction of **11**
293	354.2	451.9	0.72	300.8	0.8
298	598.2	701.3	1.02	321.8	1.0
303	806.8	1038	1.52	341.6	1.1
308	1220	1718	2.11	357.4	1.3
313	1842	2414	2.64	387.4	1.5

of L-cysteine with the palladium(II) and platinum(II) complexes **8–10** is a simple substitution process (Tables 6 and Figs. S1–S3), the reaction of L-cysteine with the gold(III) complex (**11**) was found to be initial fast, followed by a much slower process, which was attributed to reduction to gold(I) (Tables 6, Figs. S4 and S5). The substitution of the aqua ligands in **8–11** with L-cysteine can be represented by Eqs. (1) and (2)

$$[M(\mathbf{L1})(OH_2)_2]^{n+} + Cys \underset{k_{-1}}{\overset{k_{ob}}{\rightleftarrows}} [M(\mathbf{L1})(OH_2)(Cys)]^{n+} + \quad (1)$$

$$[M(\mathbf{L1})(OH_2)(Cys)]^{n+} + \underset{}{\overset{k_1}{\rightleftarrows}} [M(\mathbf{L1})(Cys)_2]^{n+} + H_2O \quad (2)$$

(M = Pd, n = 2 (**8**), Pt, n = 2 (**10**); M = Au, n = 3 (**11**); Cys = L-cysteine).

$$k_{obs} = k_{-1} + k_1[Cys] \quad (3)$$

A two-term rate equation (Eq. (3)) describes these reactions, which is typical of the direct substitution of water molecules by a nucleophile, and the reverse reaction where a water molecule replaces the coordinated nucleophile [27]. Linear plots of k_{obs} versus [Cys] for **8**, **9** and **11** with non-zero intercepts signifies reversibility of this step (Figs. 5 and 6), also observed Schmülling et al. [11] for the substitution reactions of $[PtC_6H_3X(CH_2NMe_2)(NC_5H_4SO_3^{3-})(H_2O)]$ complexes (X = H, 3-OMe) with thiourea. However, for platinum(II) complex **10** the intercept for a similar plot was insignificant (k_{-1} = 6.44 × 10^{-4} s^{-1}) (Fig. 7). The gold(III) complex **11**, was further reduced with k_{obs} and k_3 being much smaller than the corresponding values for the substitution process (Tables S4 and S5).

In general all the rates of substitution reactions of complexes **8–11** with L-cysteine were found to be pseudo first-order. Similar substitution reactions patterns with different nucleophiles have been observed for many platinum(II) compounds and a few palladium(II) compounds. For example $[Pt(bpy)(H_2O)_2]^{2+}$ (bpy = *N*,*N*′-bipyridine) [28], $[Pt(en)(H_2O)_2]^{2+}$ (en = ethylenediamine) [28] and [Pd(en)(cbdca)] (en = ethylenediamine, cbdca = cyclobutane-1,1-dicarboxylate) [29] reacts with thiourea in a similar way as observed for compounds **8–11** herein (*vide supra*). The rate constants

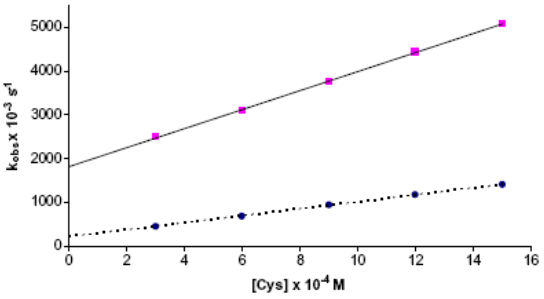

Fig. 5. Plots of k_{obs} vs. [Nu] for (a) **8** (3.8 × 10^{-5} M) (---) and (b) **9** (3.0 × 10^{-5} M) (—) at 303 K, I = 0.1 M.

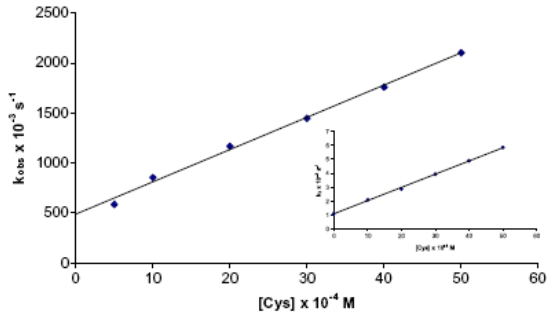

Fig. 6. Plots of k_{obs} vs. [Nu] for **11** (5.0 × 10^{-5} M) at 298 K, I = 0.1 M. Inset is the plot for the reduction process.

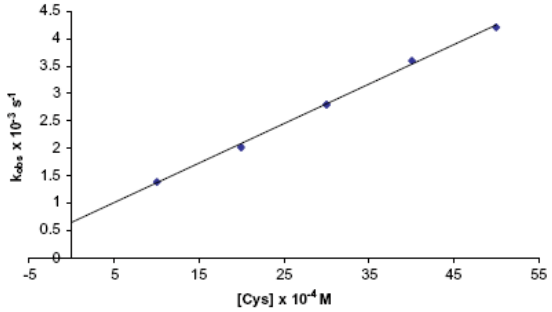

Fig. 7. Plots of k_{obs} vs. [Nu] for **10** (5.0 × 10^{-5} M) at 293 K, I = 0.1 M.

Table 7
Activation parameters determined from the temperature dependence of the rate constants for the substitution of Pd(II), Pt(II) and Au(III) complexes, and reduction of Au(III).

Activation parameters	**8**	**9**	**10**	**11**	Reduction of **11**
$\Delta H^{\ddagger}$ (kJ mol^{-1})	6.80	48.3	42.6	62.2	18.4
$\Delta S^{\ddagger}$ (J K^{-1} mol^{-1})	−47.8	18.4	−82.6	−174	−183

for the substitution reactions of L-cysteine in palladium(II) complexes **8** and **9** are faster than in platinum(II) complex **10** (Table 6). The $\Delta H^{\ddagger}$ and $\Delta S^{\ddagger}$ for these reactions are given in Table 7 and signifies these reactions proceed via an associative mechanism [27,30]. Our results generally agree with literature reports that substitution reactions of square-planar palladium(II) complexes are faster than for square-planar gold(III) and platinum(II) complexes, respectively [11,31].

Although these slow rates would suggest that **3a** would have better chance of reaching the target in cells compared to complexes **1**, **2** and **5a**, the IC_{50} values are similar for all the four compounds. This therefore suggests that the reaction of these compounds with sulfur-containing molecules in the biological *milieu* is not the determining factor in the observed anticancer activity of **1–6a** and that the low anticancer activity of complexes **1–6a** against CHO cells is intrinsic.

4. Conclusions

Bis(pyrazolyl)acetic acid compounds form neutral palladium(II), platinum(II) and gold(III) that can behave as typical carboxylic

acids. This is typified by platinum complex **3a** that readily dissociates and in the presence of potassium ions self-assembles to give a hexanuclear complex with four platinum atoms and two potassium atoms (**3b**). A strongly polarising gold(III) centre in the complex **5a** may have triggered the hydrolysis of **5a** to **5b**. All the bis(pyrazolyl)acetic acid palladium(II), platinum(II) and gold(III) complexes have low activities towards CHO cells. The substitution reaction of L-cysteine with the palladium(II) platinum(II) and gold(III) compounds suggests that kinetic labilities of these complexes and their subsequent reactions with sulfur-containing molecules in the biological milieu may not be the cause of the low activities of these complexes.

The substitution reactions of L-cysteine with the diaqua metal complexes **8–11** were found to be temperature dependent and occur *via* an associative mechanism. The reaction of **10** with L-cysteine is, however, slow compared to that of **8**, **9** and **11**. The substitution reaction with the gold(III) complex, **11**, showed a two-step reaction involving the substitution of aqua ligands and subsequent reduction to gold(I).

Acknowledgements

We acknowledge a bursary to F.K.K. by Project AuTEK (Mintek and Harmony Gold, South Africa) for providing some of the running cost for this work. We also acknowledge the Southern & Eastern African Network of Analytical Chemists (SEANAC) for a short-term fellowship to FKK for a research visit to the University of Botswana for the kinetic studies. We are grateful to Mr. Stonard Kanyanda of University of the Western Cape, South Africa for the biological screening of the compounds.

Appendix A. Supplementary material

CCDC 655155, 655156, 618083 and 655333 contain the supplementary crystallographic data for this paper. These data can be obtained free of charge from The Cambridge Crystallographic Data Centre via www.ccdc.cam.ac.uk/data_request/cif. Supplementary data associated with this article can be found, in the on-line version, at doi:10.1016/j.ica.2008.11.030.

References

[1] S. Trofimenko, Chem. Rev. 93 (1993) 943.
[2] H. Adams, S.T. Batten, G.M. Davies, M.B. Duriska, J.C. Jeffery, P. Jensen, J. Lu, G.R. Motson, S.J. Coles, M.B. Hursthouse, M.D. Ward, Dalton Trans. (2005) 1910.
[3] (a) A. Otero, J. Fernández-Baeza, A. Antiñolo, J. Tejeda, A. Lara-Sánchez, Dalton Trans. (2004) 1499;
(b) A. Otero, J. Fernández-Baeza, A. Antiñolo, J. Tejeda, A. Lara-Sánchez, L. Sánchez-Barba, A.M. Rodríguez, M.A. Maestro, J. Am. Chem. Soc. 126 (2004) 1330;
(c) A. Otero, J. Fernandez-Baeza, A. Antiñolo, J. Tejeda, A. Lara-Sánchez, L. Sánchez-Barba, M. Sanchez-Molina, S. Franco, I. Lopez-Solera, A.M. Rodríguez, Dalton Trans. (2006) 4359;
(d) A. Otero, J. Fernández-Baeza, A. Antiñolo, J. Tejeda, A. Lara-Sánchez, L. Sánchez-Barba, M.T. Expósito, A.M. Rodríguez, Dalton Trans. (2003) 1614.
[4] F. Mohr, E. Cerrada, M. Laguna, Dalton Trans. (2006) 5567.
[5] M. El-Khateeb, T.G. Appleton, L.R. Gahan, B.G. Charles, S.J. Berners-Price, A.J. Bolton, Inorg. Biochem. 77 (1999) 13.
[6] (a) S. Carotti, G. Marcon, M. Marussich, T. Mazzei, L. Messori, E. Mini, P. Orioli, Chem.-Biol. Interact. 125 (2000) 29;
(b) S. Carotti, A. Guerri, T. Mazzei, L. Messori, E. Mini, P. Orioli, Inorg. Chim. Acta 281 (1998) 90.
[7] G. Marcon, S. Carotti, M. Coronnello, L. Messori, E. Mini, P. Orioli, T. Mazzei, M.A. Cinellu, G. Minghetti, J. Med. Chem. 45 (2002) 1672.
[8] V. Milacic, D. Chen, L. Ronconi, K.R. Landis-Piwowar, D. Fregona, Q.P. Dou1, Cancer Res. 66 (2006) 10478.
[9] F.A. Cotton, G. Wilkinson, Advanced Inorganic Chemistry, 5th ed., John Wiley and Sons, New York, 1988. p. 919.
[10] R.N. Bose, S.K. Ghosh, S. Moghaddas, J. Inorg. Biochem. 65 (1997) 199.
[11] M. Schmulling, A.D. Ryabov, R. van Eldik, J. Chem. Soc., Dalton Trans. (1994) 1257.
[12] S. Elmroth, Z. Bugarcic, L.I. Elding, Inorg. Chem. 31 (1992) 3551.
[13] D. Fan, C.T. Yang, J.D. Ranford, P.F. Lee, J.J. Vittal, Dalton Trans. (2003) 2680.
[14] B.R. King, J.J. Eisch, Organometallic Syntheses, vol. 3, Elsevier Science, Publishers B.V., New York, 1986. p. 324.
[15] B.P. Block, Inorg. Synth. 4 (1953) 14.
[16] N. Burzlaff, I. Hegelmann, B. Weibert, J. Organomet. Chem. 626 (2001) 16.
[17] Bruker-AXS, SADABS V.2.05, SAINT V.6.22, SHELXTL V.6.10 and SMART 5.622 Software Reference Manuals, Bruker-AXS, Madison, Wisconsin, USA, 2000–2003.
[18] (a) H. Babich, E. Borenfreund, Appl. Environ. Microbiol. 57 (1991) 2101;
(b) H. Babich, E. Borenfreund, ATLA 18 (1991) 129.
[19] F.K. Keter, S. Kanyanda, S.S.L. Lytangaye, J. Darkwa, D.J.G. Rees, M. Meyer, Cancer Chemoth. Pharm. 63 (2008) 127.
[20] D. Jaganyi, A. Hofmann, R. van Eldik, Angew. Chem., Int. Ed. 40 (2001) 1680.
[21] E. Bulak, O. Sarper, A. Dogan, F. Lissner, T. Schleid, W. Kaim, Polyhedron 25 (2006) 2577.
[22] F.H. Allen, Acta Crystallogr., Sect. B 58 (2002) 380.
[23] V. Donald, J.G. Voet, C.W. Pratt, Fundamentals of Biochemistry, Von Hoffmann Press Inc., New York, 1999. p. 33.
[24] L. Cao, M.C. Jennings, R.J. Puddephat, Inorg. Chem. 46 (2007) 1361.
[25] J. Vicente, M.D. Bermudez, M.T. Chicote, M.J. Sanchez-Santano, J. Chem. Soc., Dalton Trans. (1990) 1945.
[26] D. Fan, C.-T. Yang, J.D. Ranford, J.J. Vittal, Dalton Trans. (2003) 4749.
[27] A. Shoukry, M. Brindell, R. van Eldik, Dalton Trans. (2007) 4169.
[28] N. Summa, W. Schiess, R. Puchta, N.V. Hommes, R. Van Eldik, Inorg. Chem. 45 (2006) 2948.
[29] A. Shoukry, T. Rau, M. Shoukry, R. van Eldik, J. Chem. Soc., Dalton Trans. (1998) 3105.
[30] H.C. Bajaj, R. van Eldik, Inorg. Chem. 27 (1988) 4052.
[31] F.A. Cotton, G. Wilkinson, Advanced Inorganic Chemistry, 6th ed., John Wiley and Sons, New York, 1988. p. 1289.